Search for Gravitational Waves from Soft Gamma Repeaters

LIGO-P070105-00-Z internal distribution only - Draft V14 - PRL target

(LIGO Scientific Collaboration + K. Hurley + others), *

(Dated: March 17, 2008)

NB: Preliminary open box draft.

We present the results of a search for short-duration gravitational waves associated with Soft Gamma Repeater (SGR) bursts using LIGO data. We find no evidence for the association of gravitational waves with any of the events in a sample including the December 2004 giant flare from SGR 1806-20 and 214 lesser bursts from SGR 1806-20 and SGR 1900+14 which occurred during the first year of LIGO's fifth science run. Gravitational wave strain upper limits and model-dependent gravitational wave emission energy upper limits have been estimated for individual bursts using a variety of simulated waveform types. The unprecedented sensitivity of the detectors allowed us to set the most stringent limits on transient gravitational wave amplitudes published to date. We find upper limit estimates on the model-dependent isotropic gravitational wave emission energies (at an assumed distance of 10 kpc) between 1.5×10^{-9} and 1.5×10^{-2} $M_{\odot}c^2$ (2.7×10^{45} and 2.7×10^{52} erg), depending on waveform type, detector antenna factors and noise characteristics at the time of the burst. These energies overlap the range of electromagnetic emission energies observed from SGR giant flare events, and future gravitational wave detectors will begin to probe SGR models using even common SGR bursts.

Soft Gamma Repeaters (SGRs) are astrophysical sources that sporadically emit brief ($\sim$ 0.1 s) intense bursts of soft gamma-rays with luminosities up to 10^{41} erg/s [1]. Less common intermediate bursts with greater peak luminosities can last for seconds. Rare 'giant flare' events, some 1000 times brighter than common bursts [2], have tails lasting minutes and are among the most electromagnetically luminous events in the Universe [1]. Of the four confirmed SGRs, three have produced a giant flare since the discovery of the first SGR in 1979 [3–5]. Under the *magnetar* model [6, 7] SGRs are neutron stars with exceptionally strong magnetic fields $\sim 10^{15}$ G [6]. Bursts result from interaction of the star's magnetic field with its solid crust, leading to crustal deformations and occasional catastrophic cracking [7, 8] with subsequent excitation of the star's nonradial modes [9–11], making SGRs interesting candidates for gravitational wave (GW) emission [10, 12]. Excitation of non-radial modes would also occur if SGRs are instead solid quark stars [12–14] as suggested to explain a discrepancy between the energy capable of being stored in a neutron star crust ($\sim 10^{44}$ erg) and the electromagnetic energy emitted by the SGR 1806-20 giant flare ($\sim 10^{46}$ erg).

We present a search for short-duration GW signals ($\lesssim$ 300 ms) associated with SGR bursts using data collected by the Laser Interferometer Gravitational Wave Observatory (LIGO) [15, 16], which consists of two colocated GW detectors at Hanford, WA with baselines of 4 km and 2 km and one 4 km detector at Livingston, LA. The SGR burst sample was provided by the gamma-ray satellites of the interplanetary network (IPN) [17], and includes the 27 December 2004 SGR 1806-20 giant flare and 214 confirmed SGR bursts occurring during the first year of LIGO's fifth science run (S5) from 14 November 2005 to 14 November 2006. The sample includes 152 SGR 1806-20 bursts (73 with three LIGO detectors observing, 42 with two detectors, 17 with a single detector, and 20 with no detector) and 62 SGR 1900+14 bursts (43 with three detectors, 12 with two detectors, 2 with a single detector, and 5 with no detector), one of which was a multi-episodic 'storm' lasting $\sim$32 s. To analyze a given SGR burst we divided GW data into an on-source time region (in which GWs associated with the burst could be expected) and a background time region (in which we do not expect an associated GW, but in which the noise is statistically similar to the on-source region). For isolated bursts the on-source region was 4 s of data centered on the SGR burst. This choice accounts for uncertainties in the geocentric electromagnetic peak time; GW emission is expected to occur almost simultaneously with the electromagnetic burst [11]. There were two special cases: 1) for two SGR 1900+14 bursts which occurred within 4 s we chose a 7 s on-source region; 2) for the SGR 1900+14 storm we chose a 40 s on-source region. Identical data quality cuts [ref] were applied to both on-source and background regions. On-source regions subject to a cut were excluded. The first 1000 s of data on either side of a given burst's on-source region surviving data quality cuts were used for the background. On-source and background segments were analyzed identically resulting in lists of *analysis events*. The background was used to estimate the significance of on-source analysis events; significant events, if any, were subject to additional environmental vetoes and consistency checks.

The analysis targeted neutron star fundamental mode ringdowns (RDs) predicted in some models [9–11, 18, 19] as well as unmodeled short-duration GW signals. The search algorithm was based on the excess power statistic [20] using a specific time window and frequency band. Frequency bands were chosen as appropriate for the target signals; time windows and clustering parameters were tuned to optimally detect the target signal. All parameters were chosen before searching the on-source region, using simulations inserted into background data. Model predictions from [21] for 10 realistic neutron star equations of state give RD frequencies in the range 1.5–3 kHz and damping times in the range 100–400 ms. We used a search frequency band 1–3 kHz for RD searches (to include some stiffer equatons of state), and found a time window of 250 ms to be optimal. The search for unmodeled signals used time windows set by prompt SGR burst timescales (5–200 ms) and frequency bands set by the detector's sensitivity. We found a time window of 125 ms optimally covered this duration range, and we searched in two frequency bands: 100–200 Hz (probing the most sensitive region of the detectors) and 100–1000 Hz (for full spectral coverage).

Model-dependent loudest event upper limits [22] on GW strain and energy were estimated for each on-source region using simulated RDs and white noise burst (WNB) signals (with frequency bands limited to the search band) for the RD and unmodeled searches, respectively [23]. Simulation parameters (frequency, decay time constant τ for RDs; duration for WNBs) were chosen to probe the respective target signal parameter spaces. Simulated detector responses [24]

$$\xi_d^{\rm sim}(t) = F_d^{+}(\theta,\phi,\psi) h_{+}^{\rm sim}(t) + F_d^{\times}(\theta,\phi,\psi) h_{\times}^{\rm sim}(t) \quad (1)$$

were constructed for each detector d and injected (with appropriate time-of-flight delays accounting for detector locations) at random times into the background. $h_{+}^{\rm sim}(t)$ and $h_{\times}^{\rm sim}(t)$ simulate incoming GW strain timeseries and $F_d^{+}(\theta,\phi,\psi)$ and $F_d^{\times}(\theta,\phi,\psi)$ are d's antenna functions calculated for source sky locations $\{\theta,\phi\}$ and polarization angles ψ [24]. The square of the root sum square (rss) strain [25] is $h_{\rm rss}^2 = h_{\rm rss+}^2 + h_{\rm rss\times}^2$, where e.g. $h_{\rm rss+}^2 = \int_{-\infty}^{\infty} h_+^2\, dt$. For simulations we choose $h_{rss+}^{\rm sim} = h_{rss\times}^{\rm sim}$. Strain upper limits discussed in this paper are estimates of the $h_{\rm rss}$ of a wave incident on the detectors.

The $h_{\rm rss}^{90\%}$ upper limit estimates correspond to GW emission energy upper limits. We assumed isotropic emission and used an assumed source distance of $R = 10$ kpc (source locations are discussed in [26, 27]. The characteristic isotropic GW emission energy $E_{GW}^{90\%}$ associated with a burst depends on the simulation waveform and can be estimated via [28]

$$E_{\rm GW} = 4\pi R^2 \frac{c^3}{16\pi G} \int_{-\infty}^{\infty} \left((\dot{h}_+)^2 + (\dot{h}_\times)^2 \right) dt, \quad (2)$$

which follows from the equation for the GW energy flux in the direction of propagation [29].

Analysis was performed by the *flare* pipeline [23, 28], which searched on-source regions for GW signals and estimated upper limits, for single detector analysis and coherent analysis with two nearly-aligned detectors such as the LIGO 4 km detectors. In the case of a triple coincident SGR burst, the flare pipeline used data from the two 4 km detectors only, and achieved sensitivity comparable to the *coherent WaveBurst* pipeline [30, 31] which included the less sensitive co-located 2 km Hanford detector as well.

Flare pipeline algorithm - Data conditioning consists of bandpassing strain-calibrated data [32] to match the search region (∼60-3500 Hz) and notching narrow lines arising from a variety of noises (such as AC power harmonics and test mass suspension modes).

Time-frequency tilings are then created for single detectors from a series of discrete Fourier transforms. In one-detector searches, the power in each tile is calculated. In two-detector searches, tiles from one detector are multiplied by the complex conjugate of corresponding tiles from the other detector, and the absolute value of the real part is taken, giving the cross power spectrum which is then treated in the same way as the auto power spectrum in a one-detector search. The off-source mean power in each frequency bin is then subtracted from tiling elements. Finally, a clustering algorithm [23, 28] applied to tiling elements produces analysis events.

Post-production consists of constructing efficiency curves by repeatedly analyzing 4 s segments, each containing a single simulation created with a range of $h_{\rm rss}^{\rm sim}$ values, and comparing the loudest simulation analysis event within 100 ms (for RDs) or 50 ms (for WNBs) of the known injection time to the loudest on-source analysis event. The $E_{GW}^{\rm sim}$ value at 90% detection efficiency ($E_{GW}^{90\%}$) occurs where 90% of the loudest simulation analysis events are larger than the loudest on-source event.

Results - No on-source analysis event was found to have a false alarm rate (estimated from the background) less than 1.4×10^{-3} Hz (1 per ∼700 s, which is consistent with the background. We thus find no evidence for the association of gravitational waves with any of the SGR burst events in the sample. We have estimated strain and energy upper limits $h_{\rm rss}^{90\%}$ and $E_{GW}^{90\%}$ using the loudest on-source analysis event for each SGR burst. Upper limits depend on search pipeline parameter tuning choices, detector sensitivity and antenna factors at the time of the burst, the loudest on-source analysis event, and the simulation waveform class used.

Table I gives upper limit estimates for two of the most interesting bursts in the sample: the 27 December 2004 SGR 1806-20 giant flare and the S5 SGR 1900+14 storm [35]. (For the complete table see [33].) At the time of the giant flare, the LIGO 4 km Hanford detector was taking data during a commissioning period under LIGO's Astrowatch program [34], and was less sensitive than during S5 by a factor of ∼3. For upper limits estimated via WNBs, two durations (11 and 100 ms) were used for simulations; other durations in the range 5–200 ms are detected using the flare pipeline with at most 20% sensitivity degradation. For RD upper limits, one value of τ (200 ms) was used. In a matched filter search, a 200 ms RD template loses at most about 10% amplitude signal-

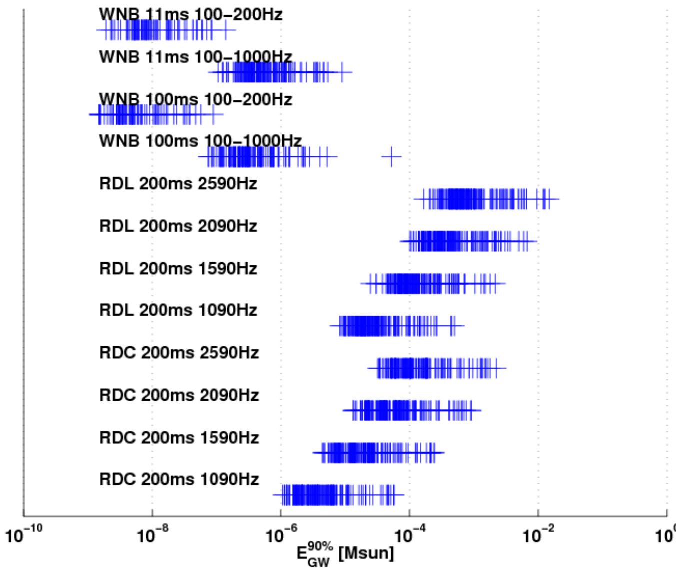

FIG. 1: [Preliminary] $E_{GW}^{90\%}$ upper limits for the SGR 1806-20 burst sample treated in the analysis. Upper limits depend on the detector network sensitivity at the time of the burst, the network antenna factor for the burst, and the loudest on-source analysis event. The limits shown in Table I, for the giant flare and S5 storm, are indicated in the figure by red diamonds and circles, respectively.

to-noise for signals in the range 100–400 ms [36]; we expect the loss to be less than this in our excess power search. RD upper limits scale roughly linearly with frequency. Superscripts in the table give one-sided 95% confidence uncertainties. The first number gives the systematic uncertainty arising from the detector calibrations, placed at 10%. The second is a statistical uncertainty arising from using a finite number of injected simulations. Uncertainties are added to the upper limit estimate. Fig. 1 shows $E_{GW}^{90\%}$ limits for the waveforms considered, for the entire sample.

Discussion - Two searches for GW associated with SGR events have been performed in the past; neither search resulted in a detection. The AURIGA collaboration searched for GW bursts associated with the SGR 1806-20 giant flare of 27 December 2004 using a method optimized for their bar detector [37]. We note that the AURIGA band (with peak sensitivity at 930 Hz [37]) is below the RD frequency range of interest. The LIGO collaboration has performed a search for long-duration GW emission associated with quasi-periodic oscillations in the SGR 1806-20 giant flare tail [38].

Upper limits $E_{GW}^{90\%}$ in the sample are in the range of electromagnetic isotropic energies E_{EM} observed from SGR giant flare events, 10^{-10} to 10^{-8} solar masses [2, 5]. Some models of SGR flares predict $E_{GW} \sim E_{EM}$ (see for example [10–12]). Table I lists upper limit results for two SGR bursts in the sample with large values of γ, where $\gamma = E_{EM}/E_{GW}^{90\%}$ is a measure of how an upper limit estimate probes the energy reservoir of the compact SGR source. Upper limits on bursts with $\gamma \sim 1$ thus probe the energy reservoir under existing theories. The Advanced LIGO detectors promise an increase in h_{rss} sensitivity by more than a factor of 10 over S5, corresponding to an increase in energy sensitivity (and therefore γ) by more than a factor of 100. Therefore even intermediate SGR bursts observed by Advanced LIGO could begin to probe to SGR models, either through detection or upper limits.

The authors gratefully acknowledge the support of the United States National Science Foundation for the construction and operation of the LIGO Laboratory and the Science and Technology Facilities Council of the United Kingdom, the Max-Planck-Society, and the State of Niedersachsen/Germany for support of the construction and operation of the GEO600 detector. The authors also gratefully acknowledge the support of the research by these agencies and by the Australian Research Council, the Council of Scientific and Industrial Research of India, the Istituto Nazionale di Fisica Nucleare of Italy, the Spanish Ministerio de Educacion y Ciencia, the Conselleria d'Economia Hisenda i Innovacio of the Govern de les Illes Balears, the Scottish Funding Council, the Scottish Universities Physics Alliance, The National Aeronautics and Space Administration, the Carnegie Trust, the Leverhulme Trust, the David and Lucile Packard Foundation, the Research Corporation, and the Alfred P. Sloan Foundation. KH is grateful for support under JPL Contracts 1282043 and 1268385, and NASA grants NAG5-11451 and NNG04GM50G. This paper is LIGO-P070105-00-Z.

* peter.kalmus@ligo.org

[1] P. M. Woods and C. Thompson, in *Compact Stellar X-Ray Sources*, edited by W. G. H. Lewin and M. van der Klis (Cambridge Univ. Press, Cambridge, 2004), astro-ph/0406133.
[2] D. M. Palmer, S. Barthelmy, N. Gehrels, R. M. Kippen, T. Cayton, C. Kouveliotou, D. Eichler, R. A. M. J. Wijers, P. M. Woods, J. Granot, et al., Nature **434**, 1107 (2005), http://arxiv.org/abs/astro-ph/0503030.
[3] E. P. Mazets et al., Nature **282**, 587 (1979).
[4] K. Hurley et al., Nature **397**, 41 (1999), astro-ph/9811443.
[5] K. Hurley et al., Nature **434**, 1098 (2005), astro-ph/0502329.
[6] R. C. Duncan and C. Thompson, Astrophys. J. Lett. **392**, L9 (1992).
[7] C. Thompson and R. C. Duncan, MNRAS **275**, 255 (1995).
[8] S. J. Schwartz, S. Zane, R. J. Wilson, F. P. Pijpers, D. R. Moore, D. O. Kataria, T. S. Horbury, A. N. Fazakerley, and P. J. Cargill, Astrophys. J. Lett. **627**, L129 (2005), http://arxiv.org/abs/astro-ph/0504056.
[9] N. Andersson and K. D. Kokkotas, Mon. Not. R. Astr.

TABLE I: [Preliminary] Energy and strain loudest event upper limit estimates at 90% detection efficiency ($E_{GW}^{90\%}$ and $h_{rss}^{90\%}$) for the SGR 1806-20 giant flare and the S5 SGR burst with the largest ratio of isotropic electromagnetic emission energy to isotropic GW emission energy, $\gamma = E_{EM}/E_{GW}^{90\%}$, for various circularly/linearly polarized RD (RDL/RDC) and WNB simulations, and 4 s and 40 s on-source regions respectively. Uncertainties (in superscripts, the first due to detector calibration, the second due to monte carlo statistics) are folded into the final upper limit estimates TBD. At the giant flare time the LIGO Hanford 4 km detector rms antenna factor for SGR 1806-20 was 0.3. The S5 SGR 1900+14 storm began at 29 March 2006 02:53:08 UTC; all three detectors were observing, with rms antenna factors for SGR 1900+14 of 0.4/0.5 for Hanford/Livingston sites.

	SGR 1806-20 Giant Flare			SGR 1900+14 storm (GCN circular 4946)		
type	$h_{rss}^{90\%}[10^{-22}\ \mathrm{Hz}^{-\frac{1}{2}}]$	$E_{GW}^{90\%}[M_\odot c^2]$	γ	$h_{rss}^{90\%}[10^{-22}\ \mathrm{Hz}^{-\frac{1}{2}}]$	$E_{GW}^{90\%}[M_\odot c^2]$	γ
WNB 11ms 100-200Hz	$18.9^{+0.0\ +0.0} = 18.9$	1.8×10^{-07}	3.1×10^{-2}	$3.67^{+0.0\ +0.0} = 3.67$	6.6×10^{-09}	1.6×10^{-5}
WNB 100ms 100-200Hz	$17.4^{+0.0\ +0.0} = 17.4$	1.5×10^{-07}	3.7×10^{-2}	$3.10^{+0.0\ +0.0} = 3.10$	4.5×10^{-09}	2.4×10^{-5}
WNB 11ms 100-1000Hz	$56.7^{+0.0\ +0.0} = 56.7$	2.0×10^{-05}	2.8×10^{-4}	$10.9^{+0.0\ +0.0} = 10.9$	7.1×10^{-07}	1.5×10^{-7}
WNB 100ms 100-1000Hz	$44.3^{+0.0\ +0.0} = 44.3$	1.1×10^{-05}	5.1×10^{-4}	$8.84^{+0.0\ +0.0} = 8.84$	4.4×10^{-07}	2.4×10^{-7}
RDC 200ms 1090Hz	$60.1^{+0.0\ +0.0} = 60.1$	9.0×10^{-05}	6.2×10^{-5}	$12.5^{+0.0\ +0.0} = 12.5$	3.9×10^{-06}	2.7×10^{-8}
RDC 200ms 1590Hz	$88.3^{+0.0\ +0.0} = 88.3$	4.1×10^{-04}	1.4×10^{-5}	$16.2^{+0.0\ +0.0} = 16.2$	1.8×10^{-05}	5.9×10^{-9}
RDC 200ms 2090Hz	$112^{+0.0\ +0.0} = 112$	1.1×10^{-03}	5.1×10^{-6}	$21.4^{+0.0\ +0.0} = 21.4$	4.0×10^{-05}	2.7×10^{-9}
RDC 200ms 2500Hz	$150^{+0.0\ +0.0} = 150$	2.9×10^{-03}	1.9×10^{-6}	$28.1^{+0.0\ +0.0} = 28.1$	1.0×10^{-04}	1.1×10^{-9}
RDL 200ms 1090Hz	$186^{+0.0\ +0.0} = 186$	8.6×10^{-04}	6.5×10^{-6}	$38.8^{+0.0\ +0.0} = 38.8$	3.7×10^{-05}	2.9×10^{-9}
RDL 200ms 1590Hz	$281^{+0.0\ +0.0} = 281$	4.1×10^{-03}	1.4×10^{-6}	$50.8^{+0.0\ +0.0} = 50.8$	1.3×10^{-04}	8.2×10^{-10}
RDL 200ms 2090Hz	$461^{+0.0\ +0.0} = 461$	1.9×10^{-02}	2.9×10^{-7}	$70.9^{+0.0\ +0.0} = 70.9$	4.4×10^{-04}	2.4×10^{-10}
RDL 200ms 2500Hz	$444^{+0.0\ +0.0} = 444$	2.6×10^{-02}	2.2×10^{-7}	$86.8^{+0.0\ +0.0} = 86.8$	9.9×10^{-04}	1.1×10^{-10}

Soc. **299**, 1059 (1998), gr-qc/9711088.

[10] J. A. de Freitas Pacheco, Astronomy and Astrophysics **336**, 397 (1998), astro-ph/9805321.

[11] K. Ioka, Monthly Notices of the RAS **327**, 639 (2001), astro-ph/0009327.

[12] J. E. Horvath, Modern Physics Letters A **20**, 2799 (2005).

[13] R. X. Xu, Astrophys. J. Lett. **596**, L59 (2003), astro-ph/0302165.

[14] B. J. Owen, Physical Review Letters **95**, 211101 (2005), astro-ph/0503399.

[15] LIGO Scientific Collaboration, LIGO Internal Note P070082-02 (2007).

[16] S. A. Hughes, S. Marka, P. L. Bender, and C. J. Hogan, ECONF C **010630**, 402 (2001).

[17] ssl.berkeley.edu/ipn3.

[18] B. L. Schumaker and K. S. Thorne, Mon. Not. R. Astr. Soc. **203**, 457 (1983).

[19] N. Andersson, Classical and Quantum Gravity **20**, 105 (2003), http://arxiv.org/abs/astro-ph/0211057.

[20] W. G. Anderson, P. R. Brady, J. D. Creighton, and É. É. Flanagan, Phys. Rev. D **63**, 042003 (2001), gr-qc/0008066.

[21] O. Benhar, V. Ferrari, and L. Gualtieri, Phys. Rev. D **70**, 124015 (2004), arXiv:astro-ph/0407529.

[22] P. R. Brady, J. D. E. Creighton, and A. G. Wiseman, ArXiv General Relativity and Quantum Cosmology e-prints (2004), gr-qc/0405044.

[23] P. Kalmus, LIGO note T060120-00-Z (2006), CVS version tag ‘open’ was used for this analysis.

[24] K. S. Thorne, in *300 Years of Gravitation*, edited by S. W. Hawking and W. Israel (Cambridge University Press, Cambridge, 1987), p. 417.

[25] The LIGO Scientific Collaboration, Phys. Rev. D **72**, 062001 (2005).

[26] K. Hurley, C. Kouveliotou, T. Cline, E. Mazets, S. Golenetskii, D. D. Frederiks, and J. van Paradijs, Astrophysical Journal, Letters **523**, L37 (1999), astro-ph/9906020.

[27] D. A. Frail, S. R. Kulkarni, and J. S. Bloom, Nature **398**, 127 (1999).

[28] P. Kalmus, R. Khan, L. Matone, and S. Marka, Class. Quantum Grav. **24**, S659 (2007), astro-ph/0602402.

[29] S. Shapiro and S. Teukolsky, *Black Holes, White Dwarfs, and Neutron Stars* (Wiley, New York, 1983).

[30] S. Klimenko, LIGO note T060282-00-Z (2006).

[31] S. Klimenko, I. Yakushin, and G. Mitselmakher, LIGO note T060112-00-Z (2006).

[32] X. Siemens, B. Allen, J. Creighton, M. Hewitson, and M. Landry, ArXiv General Relativity and Quantum Cosmology e-prints (2004), gr-qc/0405070.

[33] See EPAPS Document No. XX for complete table. For more information on EPAPS, see http://www.aip.org/pubservs/epaps.html.

[34] F. Raab, LIGO Internal Note G050122 (2005), www.ligo.caltech.edu/docs/G/G050122-00/G050122-00.pdf.

[35] S. Golenetskii et al., GRB Coordinates Network **4946**, 1 (2006).

[36] J. D. E. Creighton, Phys. Rev. **D60**, 022001 (1999), gr-qc/9901084.

[37] L. Baggio, M. Bignotto, M. Bonaldi, M. Cerdonio, L. Conti, M. de Rosa, P. Falferi, P. Fortini, M. Inguscio, N. Liguori, et al., Physical Review Letters **95**, 081103 (2005), http://arxiv.org/abs/astro-ph/0506142.

[38] The LIGO Scientific Collaboration, Phys. Rev. D (2007), astro-ph/0703419.